European Radiology (2019) 29:3467–3479
https://doi.org/10.1007/s00330-019-06122-x

NEURO

Comparison of T1 mapping and fixed T1 method for dynamic contrast-enhanced MRI perfusion in brain gliomas

G. M. Conte[1] · L. Altabella[1] · A. Castellano[1] · V. Cuccarini[2] · A. Bizzi[2] · M. Grimaldi[3] · A. Costa[4] · M. Caulo[5] · A. Falini[1] · N. Anzalone[1]

Received: 9 October 2018 / Revised: 14 January 2019 / Accepted: 22 February 2019 / Published online: 10 April 2019

Abstract

Objectives To compare dynamic contrast-enhanced MRI (DCE-MRI) data obtained using different prebolus T1 values in glioma grading and molecular profiling.

Methods We retrospectively reviewed 83 cases of gliomas: 46 lower-grade gliomas (LGG; grades II and III) and 37 high-grade gliomas (HGG; grade IV). DCE-MRI maps of plasma volume fraction (Vp), extravascular-extracellular volume fraction (Ve), and tracer transfer constant from plasma to tissue (K^{trans}) were obtained using a fixed T1 value of 1400 ms and a measured T1 obtained with variable flip angle (VFA). Tumour segmentations were performed and first-order histogram parameters were extracted from volumes of interest (VOIs) after co-registration with the perfusion maps. The two methods were compared using Wilcoxon matched-pairs signed-rank test and Bland-Altman analysis. Diagnostic accuracy was obtained and compared using ROC curve analysis and DeLong's test.

Results Perfusion parameters obtained with the fixed T1 value were significantly higher than those obtained with the VFA. As regards diagnostic accuracy, there were no significant differences between the two methods both for glioma grading and molecular classification, except for few parameters of both methods.

Conclusions DCE-MRI data obtained with different prebolus T1 are not comparable and the definition of a prebolus T1 by T1 mapping is not mandatory since it does not improve the diagnostic accuracy of DCE-MRI.

Key Points

- *DCE-MRI data obtained with different prebolus T1 are significantly different, thus not comparable.*
- *The definition of a prebolus T1 by T1 mapping is not mandatory since it does not improve the diagnostic accuracy of DCE-MRI for glioma grading.*
- *The use of a fixed T1 value represents a valid alternative to T1 mapping for DCE-MRI analysis.*

Keywords Magnetic resonance imaging · Brain · Glioma · Perfusion imaging

A. Falini and N. Anzalone contributed equally to this work.

Electronic supplementary material The online version of this article (https://doi.org/10.1007/s00330-019-06122-x) contains supplementary material, which is available to authorized users.

✉ N. Anzalone
anzalone.nicoletta@hsr.it

[1] Neuroradiology Unit and CERMAC, Vita-Salute San Raffaele University and IRCCS San Raffaele Scientific Institute, Via Olgettina 60, 20132 Milan, Italy

[2] Neuroradiology Unit, Fondazione IRCCS Istituto Neurologico Carlo Besta, Milan, Italy

[3] Department of Radiology, Humanitas Clinical and Research Hospital, Rozzano, Milan, Italy

[4] Department of Neuroradiology, Fondazione IRCCS Cà Granda Ospedale Maggiore Policlinico, Milan, Italy

[5] Department of Neuroscience and Imaging and ITAB-Institute of Advanced Biomedical Technologies, University G. D'Annunzio, Chieti, Italy

Abbreviations

HGG	High-grade gliomas
IDH	Isocitrate dehydrogenase
K^{trans}	Tracer transfer constant from plasma to tissue
LGG	Lower-grade gliomas
Ve	Extravascular-extracellular volume fraction
VFA	Variable flip angle
Vp	Plasma volume fraction

Introduction

Dynamic contrast-enhanced magnetic resonance imaging (DCE-MRI) has proven to be a useful diagnostic tool in the study of brain tumours and in particular in glioma grading since it allows the characterisation of the microvascular environment of both normal and tumoural tissues [1–8]. It relies on the acquisition of T1-weighted images before, during, and after the passage of a bolus of contrast agent (CA). This generates a signal-time curve that is converted in a CA concentration-time curve in order to calculate quantitative perfusion metrics from a pharmacokinetic model. To do so, it is necessary to measure the T1 signal before the administration of the CA (prebolus T1) in order to obtain a map of pre-contrast T1 values across all the acquired volume (T1 mapping). This measurement will then be used to convert the signal intensity units (SI) in the DCE-MRI data into unit of CA concentration.

There are concerns regarding the variability and reproducibility of DCE-MRI data, mainly due to the lack of standardisation of the technique that results in the publication of different acquisition and processing protocols [9–11]. Some of the variables that can affect the reproducibility of DCE-MRI are the vascular input function selection, the software used for data analysis, and the prebolus T1 estimation method [8–12]. Nevertheless, different research groups have independently achieved relatively high diagnostic accuracy in different clinical tasks, including glioma grading, follow-up, and differential diagnosis [1–6].

One of the differences among the studies is the method chosen to measure the prebolus T1 that can be done using inversion recovery (IR), saturation recovery (SR), or variable flip angle (VFA) sequences [8, 13–16]. The most accurate method is the IR approach, but it is time-consuming and not feasible in clinical practice. VFA sequences overcome this limitation acquiring two or more spoiled gradient echo measurements with constant repetition time (TR) and echo time (TE), and different flip angles [17]. This made the VFA the most widely used approach since it requires shorter acquisition time favouring its clinical use [8].

However, VFA can potentially introduce variability and errors in perfusion measurements, mainly because of motion artefacts and B1 field inhomogeneity [8]. Even though the possibility to correct for B1 inhomogeneity exists, it is time-consuming and does not achieve complete correction, making it hardly feasible in clinical practice [8].

For this reason, the use of a fixed T1 value has been proposed as a valid alternative to T1 mapping in glioma studies [8, 18, 19]. Nevertheless, the majority of the published studies performed the T1 mapping [1, 2, 5] rather than applying a fixed T1 value [3, 4, 6] and only a few compared the two methods on the same dataset, mainly on simulated or follow-up data [8, 18, 19].

To the best of our knowledge, the only study that compared the VFA and the fixed T1 value approach in glioma grading enrolled a relatively small cohort of patients, mainly composed by glioblastoma [8].

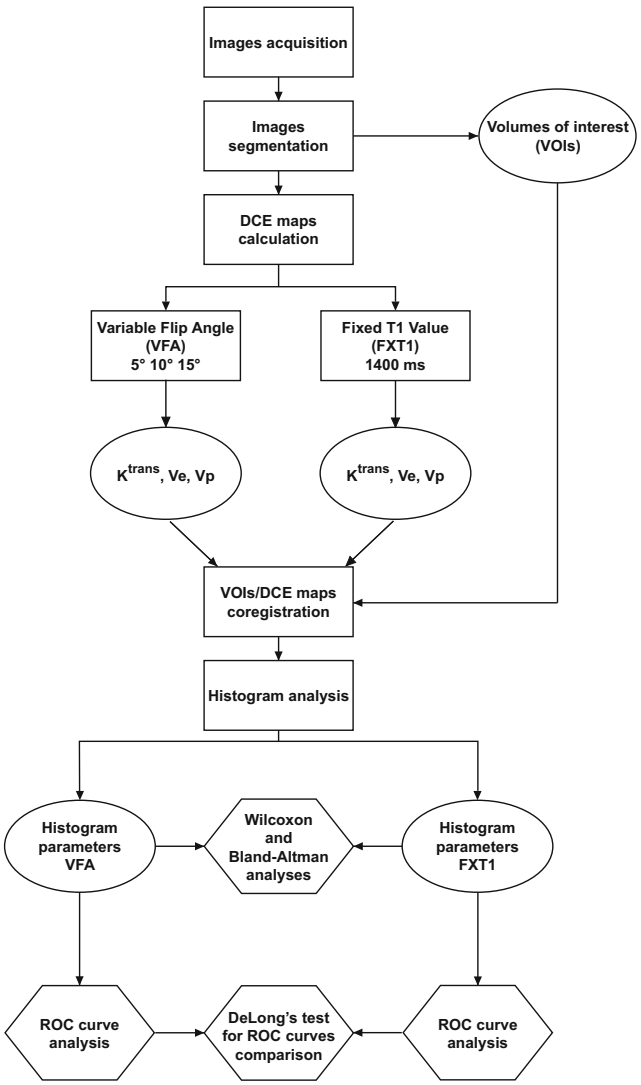

Fig. 1 Workflow showing the study design. DCE-MRI, dynamic contrast-enhanced MRI; Vp, plasma volume; K^{trans}, volume transfer constant; Ve, volume of the extravascular-extracellular space

Therefore, this study aimed to compare the diagnostic accuracy of DCE-MRI in defining glioma grade and molecular profile using metrics obtained with VFA T1 mapping and a fixed T1 value on a cohort of patients representative of all glioma grades.

Material and methods

A workflow of the study design is shown in Fig. 1.

Patients

This retrospective study involved 83 patients (mean age 52 years; range 20–80 years; 48 men, 35 women) with histologically confirmed gliomas: 46 lower-grade gliomas (LGG) and 37 high-grade gliomas (HGG); the LGG group included 23 WHO grade II and 23 WHO grade III gliomas; the HGG group included 37 WHO grade IV glioblastomas (GBMs).

Patients were selected among a cohort who performed preoperative MRI between June 2012 and June 2015 in five centres [1]. The local research ethics committees of all centres approved the study, and all patients provided signed informed consent before MR imaging. Exclusion criteria were the presence of a severe renal failure assessed by serum creatinine and a known allergy to gadolinium-based contrast agent. In each centre, an experienced neuropathologist provided the histopathologic diagnosis according to the WHO 2016 classification [20].

In 70 of the total cohort of patients (41 LGG and 29 HGG), an integrated molecular analysis was provided, including immunohistochemistry and DNA sequencing to detect isocitrate dehydrogenase (IDH) mutations and fluorescence in situ hybridisation to detect 1p/19q codeletion. In these patients, 39% (16 of 41) of the lower-grade II and III gliomas were IDH mutant (IDH-mut) and 1p/19q codeleted, 32% (13 of 41) were IDH-mut without 1p/19q codeletion, and 29% (12 of 41) were IDH wild-type (IDH-wt). Of the 29 GBMs with molecular characterisation, 28 were IDH-wt (97%).

Table 1 Imaging parameters of MRI acquisition protocol

Acquisition order	Sequence	TR (ms)	TE (ms)	TI (ms)	Flip angle	No. of dynamics	Reconstruction matrix	FOV	Thickness (mm)	Acquisition time
Philips										
1	Axial T2W Turbo SE	3000	80	–	90°	–	512 × 512	230 × 230	5	1 min 54 s
2	Axial 3D-FLAIR Turbo SE	10,000	110	2750	90°	–	256 × 256	230 × 230	2.5	8 min 20 s
3	Axial 3D spoiled gradient echo T1W	7.2	3.5	–	8°	–	256 × 256	256 × 256	2.5	1 min 22 s
4	Axial spoiled gradient echo variable flip angle (VFA)	3.9	1.9	–	5°–10°–15°	–	112 × 112	230 × 230	2.5	2 min 3 s
5	Axial Dynamic Contrast Enhanced 3D spoiled gradient echo T1W (DCE)	3.9	1.8	–	15°	70	112 × 112	230 × 230	2.5	6 min 10 s
6	Axial Dynamic Susceptibility Contrast FFE-EPI T2*W (DSC)	1500	40	–	75°	80	112 × 112	230 × 230	5	2 min 4 s
7	Post-contrast axial 3D spoiled gradient echo T1W	7.2	3.5	–	8°	–	512 × 512	256 × 256	2.5	1 min 22 s
Siemens										
1	Axial T2W Turbo SE	5000	79	–	90°	–	512 × 512	230 × 230	5	1 min 50 s
2	Axial 3D-FLAIR Turbo SE	5500	502	1800	90°	–	256 × 256	230 × 230	1	7 min 42 s
3	Axial 3D spoiled gradient echo T1W	1800	2.7	–	9°	–	256 × 256	256 × 256	2.5	5 min 47 s
4	Axial spoiled gradient echo variable flip angle (VFA)	3.9	1.9	–	5°–10°–15°	–	112 × 112	230 × 230	2.5	2 min 3 s
5	Axial Dynamic Contrast Enhanced 3D spoiled gradient echo T1W (DCE)	3.9	1.8	–	15°	70	112 × 112	230 × 230	2.5	6 min
6	Axial Dynamic Susceptibility Contrast FFE-EPI T2*W (DSC)	1500	31	–	75°	80	112 × 112	230 × 230	5	2 min 8 s
7	Post-contrast axial 3D spoiled gradient echo T1W	1800	2.7	–	9°	–	256 × 256	256 × 256	2.5	5 min 47 s

MR imaging protocol

MR imaging was performed applying a standardised acquisition protocol in five centres (Table 1). All centres had a 3.0-T MR system (Philips Healthcare and Siemens Healthcare). DCE-MRI was performed with a dynamic gradient echo T1-weighted sequence using the following parameters: TR 3.9 ms, TE 1.8 ms, flip angle 15°, matrix 112 × 112, field of view (FOV) 230 × 230 mm, section thickness 2.5 mm, in-plane acquisition voxel size 2.05 × 2.05 mm. Seventy dynamic scans were performed with a temporal resolution of 5.1 s. The total acquisition time for DCE-MRI was 6 min and 10 s. DCE-MRI was preceded by a VFA axial sequence for T1 mapping (see the 'Prebolus T1 estimation' section).

A fixed dose of 10 ml of gadobutrol (Gadovist, 1 mmol/ml; Bayer) was administered, split into two boluses of 5 ml. The first bolus of 5 ml was injected 50 s after the start of the DCE-MRI sequence using a power injector (Spectris Solaris MR injector, MedRad) at a rate of 2 ml/s, immediately followed by a 20 ml saline flush at the same injection rate. A second bolus was administered for dynamic susceptibility contrast MRI sequences, also included in the acquisition protocol but not considered in this study.

Prebolus T1 estimation

Prebolus T1 was defined using both T1 mapping and a fixed T1 value. T1 mapping was performed using VFA axial spoiled gradient echo sequences with the following parameters: TR 3.9 ms, TE 1.9 ms, flip angle 5–10–15°, number of signal averages 2, acquisition matrix 112 × 112, FOV 230 × 230, section thickness 2.5 mm, in-plane acquisition voxel size 2.05 × 2.05 mm, acquisition time 2 min 3 s.

For the analysis without the VFA, the fixed T1 value was set to 1400 ms.

Perfusion analysis

Perfusion MR analysis was performed using Olea Sphere (v. 3.0, Olea Medical Solutions). Pre-processing steps included automatic motion correction by a rigid-body registration, automatic spatial smoothing, and background segmentation. The vascular input function (VIF) was automatically measured using a tool implemented in the software [21]. Parametric maps of volume transfer constant (K^{trans}), plasma volume (Vp), and volume of the extravascular-extracellular space (Ve) were calculated using the two-compartment extended Tofts model [22] and applying the two prebolus T1 estimation

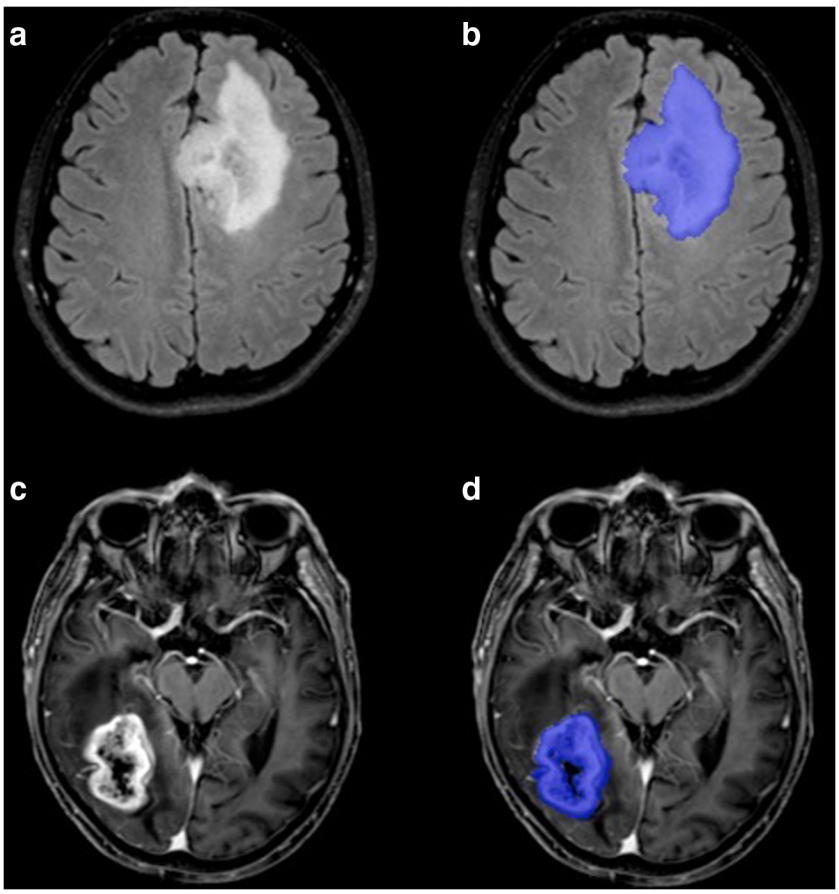

Fig. 2 Examples of segmentations. Volumes of interest were obtained segmenting FLAIR hyperintensity or the enhancing part of the tumour. The figure shows segmentations obtained for a WHO grade II diffuse astrocytoma (**a**, **b**) and a WHO grade IV glioblastoma (**c**, **d**)

Table 2 Median values of perfusion parameters and results of Wilcoxon matched-pairs signed-rank test. *LGG*, lower-grade gliomas; *HGG*, high-grade gliomas; *VFA*, variable flip angle; *Vp*, plasma volume; K^{trans}, volume transfer constant; *Ve*, volume of the extravascular-extracellular space; *IQR*, interquartile range

Parameter	LGG (WHO II and III; $n = 46$)			HGG (WHO IV; $n = 37$)		
	Fixed T1	VFA	*p* value	Fixed T1	VFA	*p* value
Vp (%)						
Mean	3.944	0.789	< 0.0001	9.784	1.700	< 0.0001
Median	2.781	0.590	< 0.0001	8.850	1.520	< 0.0001
IQR	2.719	0.501	< 0.0001	6.095	1.107	< 0.0001
5th percentile	0.562	0.099	< 0.0001	1.887	0.526	< 0.0001
10th percentile	1.015	0.165	< 0.0001	3.325	0.719	< 0.0001
25th percentile	1.765	0.319	< 0.0001	5.724	1.067	< 0.0001
75th percentile	4.545	0.921	< 0.0001	11.860	2.165	< 0.0001
90th percentile	7.761	1.389	< 0.0001	15.380	2.947	< 0.0001
95th percentile	11.01	2.023	< 0.0001	18.910	3.419	< 0.0001
K^{trans} (min^{-1})						
Mean	0.006	0.002	< 0.0001	0.094	0.021	< 0.0001
Median	0.001	0.001	0.0005	0.087	0.019	< 0.0001
IQR	0.005	0.002	0.0008	0.091	0.015	< 0.0001
5th percentile	0.000	0.000	0.0192	0.001	0.000	0.0039
10th percentile	0.000	0.000	0.0060	0.006	0.002	0.0007
25th percentile	0.000	0.000	0.0132	0.034	0.007	< 0.0001
75th percentile	0.005	0.002	0.0005	0.138	0.028	< 0.0001
90th percentile	0.013	0.006	< 0.0001	0.202	0.036	< 0.0001
95th percentile	0.022	0.009	< 0.0001	0.238	0.043	< 0.0001
Ve (%)						
Mean	1.833	0.629	< 0.0001	27.03	6.713	< 0.0001
Median	0.211	0.059	0.0048	25.08	5.666	< 0.0001
IQR	1.035	0.443	0.0015	24.30	5.854	< 0.0001
5th percentile	0	0	0.0449	0.096	0.027	0.0063
10th percentile	0	0	0.5571	0.400	0.097	0.0012
25th percentile	0.010	0.005	0.5312	7.470	2.301	0.0003
75th percentile	1.064	0.452	0.0024	37.65	9.783	< 0.0001
90th percentile	3.863	1.192	0.0002	48.87	14.15	< 0.0001
95th percentile	6.259	2.203	0.0002	61.83	16.82	< 0.0001

methods. DCE-derived parametric maps were then coregistered to the anatomic datasets using rigid transformation.

Image analysis

Segmentations were performed on post-contrast T1-weighted images for enhancing tumours and on FLAIR images for non-enhancing tumours, avoiding cystic or necrotic regions. All segmentations were performed semi-automatically with a tool implemented in the software used for perfusion analysis by a resident with 5 years of experience under the supervision of the senior author with more than 20 years of experience (N.A.) and stored as volumes of interest (VOIs) (Fig. 2). This segmentation approach examines neighbouring voxels of an initial seed point/voxel selected by the user and determines whether the voxel neighbours should be added to the region. This process is iterated as long as the user does not stop it or some algorithm fixed conditions have not been reached. Thus, the user can control this process and decide when to stop the growth of the segmentation.

The VOIs were then coregistered with the perfusion maps obtained with the two prebolus T1 maps (both that from the VFA sequence and that from the assumed map) to make the type of prebolus T1 measurement the only variable between the two datasets. For each patient and each perfusion map, first-order histogram parameters were extracted from the coregistered VOIs, including the mean, median, interquartile range, and 5th, 10th, 25th, 75th, 90th, and 95th percentile values.

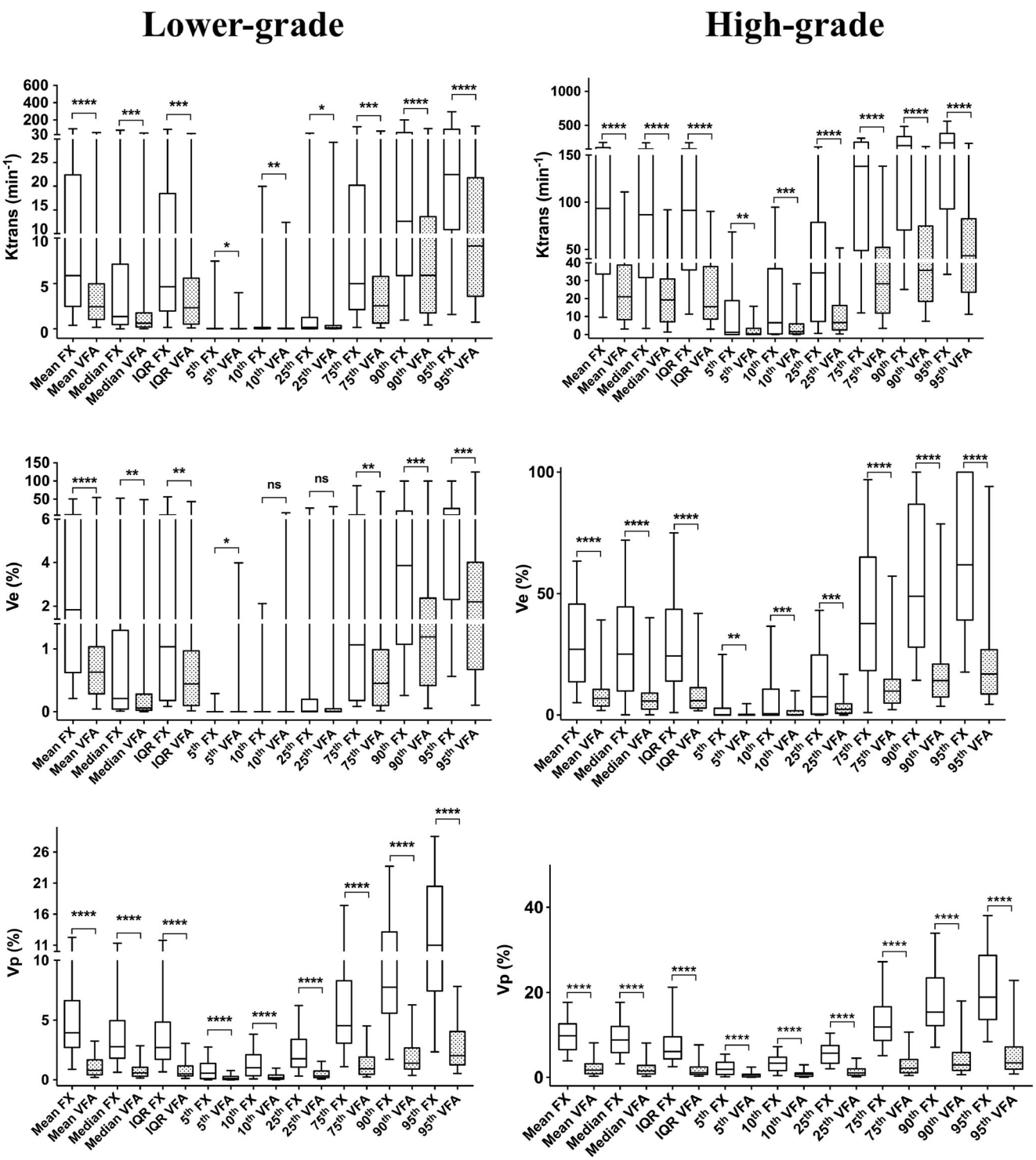

Fig. 3 Boxplots show values of K^{trans}, Ve, and Vp for lower-grade gliomas and high-grade gliomas obtained with the fixed T1 method (FX, blank) and the variable flip angle method (VFA, dotted). Median values of each histogram parameter were compared with the Wilcoxon matched-pairs signed-rank test. K^{trans} values are scaled of a factor 1000 for better visualisation. Vp, plasma volume; K^{trans}, volume transfer constant; Ve, volume of the extravascular-extracellular space

Statistical analysis

Statistical analysis was performed using Graph Pad Prism (Graph Pad), MATLAB (The MathWorks Inc.), and MedCalc (MedCalc).

To assess the distribution of the perfusion parameters measured inside the VOIs, test for normality was performed on the histogram parameters using the D'Agostino and Pearson test.

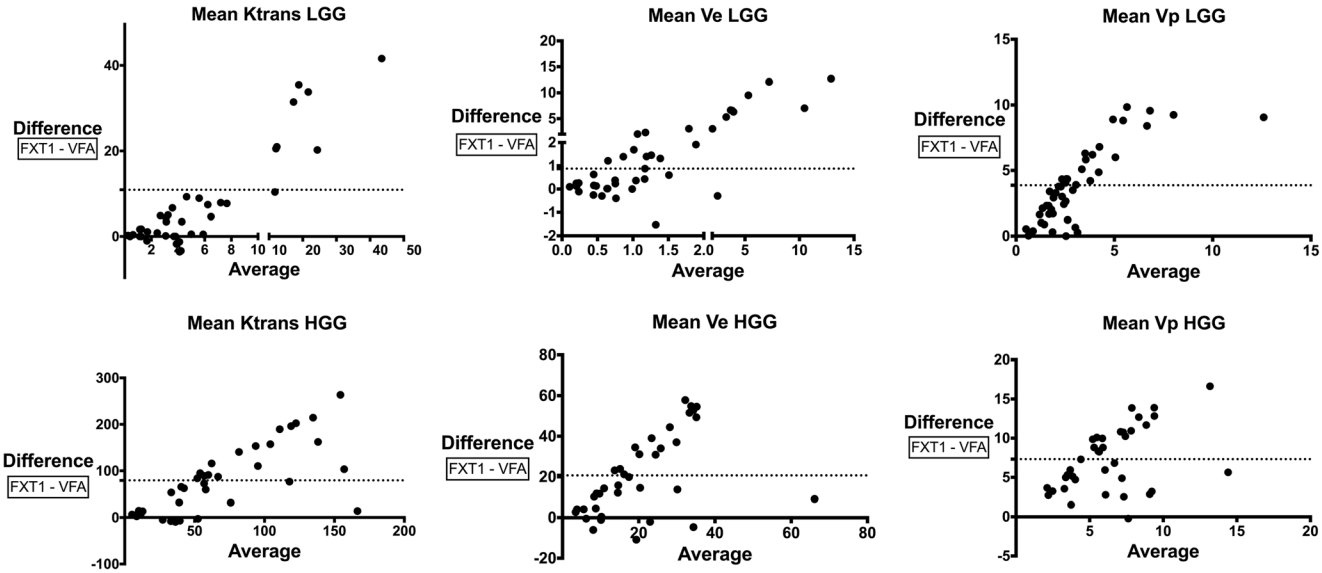

Fig. 4 Example of graphs obtained with the Bland-Altman analisys in lower-grade gliomas and high-grade gliomas. Each dot represents a patient; on the *x*-axis the average and on the *y*-axis the differences of the measurement obtained with the two prebolus T1 methods. The dotted line represents the bias. Vp, plasma volume; K^{trans}, volume transfer constant; Ve, volume of the extravascular-extracellular space; VFA, variable flip angle; FXT1, fixed T1 value; LGG, lower-grade gliomas; HGG, high-grade gliomas. For other graphs, see Electronic Supplementary Material 1–6

The perfusion parameters obtained using the T1 mapping and the fixed T1 value were compared using the Wilcoxon matched-pairs signed-rank test and Bland-Altman analysis. For these tests, LGG and HGG were analysed independently in order to avoid confounding factor due to the different scales of the perfusion parameters of the two gliomas groups.

The diagnostic accuracy of the two methods in defining glioma grade and molecular profile was obtained with ROC curve analysis and compared with DeLong's test for correlated ROC curves.

For all tests, values of $p < 0.05$ were considered statistically significant.

Results

The test for normality resulted in a non-normal distribution of the perfusion parameters extracted from the VOIs; hence, non-parametric tests were applied for further analyses.

The results of the Wilcoxon matched-pairs signed-rank test are summarised in Table 2 and Fig. 3. We found statistically significant differences for all perfusion metrics and all the histogram parameters except for the 10th and 25th percentile measurements of Ve in the LGG group. We found statistically significant differences for all comparisons in the HGG group.

Bland-Altman analyses revealed positive biases between the fixed T1 and the T1 mapping groups for all measures except for the 5th and 10th percentiles of Ve in the LGG group (Fig. 4 and Electronic Supplementary Material 1–6).

Results of ROC curve analysis are summarised in Tables 3 and 4.

In distinguishing lower-grade gliomas from GBM according to the WHO 2016 classification, the area under the curve (AUC) ranged from 0.690 to 0.918 (Table 3); a significantly higher accuracy for the median value of the Vp obtained with the fixed T1 value was found (0.870 vs. 0.778, $p = 0.0434$, DeLong's test) (Table 3).

In separating WHO grade II from grade III gliomas, the AUC ranged from 0.520 to 0.762 (Table 3); a significantly higher accuracy for the 5th and 10th values of the Ve obtained with VFA was obtained (0.543 vs. 0.674, $p = 0.0240$; 0.569 vs. 679, $p = 0.0156$ respectively) (Table 3). As for distinction of WHO grade III from grade IV gliomas, the AUC ranged from 0.618 to 0.868 (Table 3); a significantly higher accuracy for the 90th and 95th percentile values of the K^{trans} obtained with the fixed T1 value was found (0.854 vs. 0.761, $p = 0.0469$; 0.845 vs. 0.732, $p = 0.0401$ respectively) (Table 3).

Finally, in differentiating WHO grade II from grade III + IV gliomas, the AUC ranged from 0.632 to 0.893 (Table 3); a significantly higher accuracy for the 10th and 25th percentile values of the Ve obtained with the VFA was found (0.693 vs. 0.781, $p = 0.0065$; 0.736 vs. 0.839, $p = 0.0160$ respectively) (Table 3).

Regarding molecular profiling, in separating IDH-wt from IDH-mut tumours, the AUC ranged from 0.503 to 0.625 (Table 4); a significantly higher accuracy for the 5th percentile value of the Ve obtained with the fixed T1 value was found (0.625 vs. 0.506, $p = 0.0267$) (Table 4). In distinguishing IDH-

Table 3 Diagnostic accuracy of DCE in glioma grading: ROC curve analysis and comparison. *AUC*, area under the curve; *VFA*, variable flip angle; *Vp*, plasma volume; K^{trans}, volume transfer constant; *Ve*, volume of the extravascular-extracellular space; *IQR*, interquartile range

Parameter	LGG ($n = 46$) vs HGG ($n = 37$) (AUC)		AUC comparison DeLong's test (p values)	Grade II ($n = 23$) vs Grade III ($n = 23$) (AUC)		AUC comparison DeLong's test (p values)	Grade III ($n = 23$) vs Grade IV ($n = 37$) (AUC)		AUC comparison DeLong's test (p values)	Grade II ($n = 23$) vs Grade III + IV ($n = 60$) (AUC)		AUC comparison DeLong's test (p values)
	Fixed T1	VFA		Fixed T1	VFA		Fixed T1	VFA		Fixed T1	VFA	
Vp												
Mean	.837	.739	.0686	.607	.671	.5435	.776	.633	.1057	.778	.749	.6911
Median	.870	.778	.0434	.647	.709	.5340	.806	.697	.0629	.806	.788	.7898
IQR	.797	.749	.3763	.618	.705	.3814	.730	.652	.2790	.777	.789	.8555
5th percentile	.762	.748	.6825	.562	.597	.5861	.740	.712	.4828	.652	.668	.7053
10th percentile	.813	.778	.4113	.561	.614	.4866	.776	.726	.3270	.693	.713	.7022
25th percentile	.860	.782	.0701	.614	.664	.5907	.805	.713	.0965	.762	.754	.8932
75th percentile	.858	.770	.0814	.639	.713	.4730	.794	.676	.0817	.809	.799	.8806
90th percentile	.808	.734	.1966	.582	.690	.3102	.751	.652	.1715	.758	.763	.9447
95th percentile	.742	.690	.4271	.559	.665	.3263	.697	.618	.3257	.700	.720	.8024
K^{trans}												
Mean	.901	.901	1.000	.698	.752	.5496	.855	.793	.1683	.848	.873	.6400
Median	.918	.898	.3912	.647	.743	.2814	.868	.818	.1802	.833	.878	.3325
IQR	.906	.867	.2279	.679	.745	.4516	.861	.771	.0555	.845	.877	.4997
5th percentile	.733	.753	.7241	.520	.571	.6065	.711	.712	.9844	.632	.699	.2863
10th percentile	.808	.833	.6488	.550	.645	.3056	.764	.772	.8826	.701	.778	.1933
25th percentile	.912	.886	.3457	.588	.698	.2102	.863	.814	.1589	.794	.831	.4595
75th percentile	.911	.880	.2701	.681	.745	.4639	.863	.790	.0966	.849	.880	.4872
90th percentile	.899	.856	.2079	.701	.762	.5055	.854	.761	.0469	.851	.875	.6518
95th percentile	.885	.829	.1718	.703	.754	.5930	.845	.732	.0401	.841	.859	.7691
Ve												
Mean	.895	.871	.3222	.679	.739	.4889	.812	.752	.1656	.864	.893	.4288
Median	.862	.868	.8318	.646	.733	.3169	.793	.754	.3662	.796	.869	.1196
IQR	.876	.866	.7479	.709	.711	.9821	.794	.736	.2544	.863	.886	.5397
5th percentile	.765	.734	.4236	.543	.674	.0240	.751	.657	.0725	.680	.717	.2324
10th percentile	.799	.816	.6720	.569	.679	.0156	.772	.718	.2734	.693	.781	.0065
25th percentile	.833	.851	.6013	.607	.709	.1736	.780	.739	.3310	.736	.839	.0160
75th percentile	.876	.873	.9000	.711	.719	.9207	.792	.746	.3127	.862	.890	.4688
90th percentile	.883	.861	.4128	.679	.728	.5493	.786	.731	.2511	.866	.891	.4812
95th percentile	.881	.848	.2795	.667	.709	.6086	.786	.724	.2513	.859	.871	.7662

Table 4 Diagnostic accuracy in molecular profiling: ROC curve analysis and comparison. *IDH*, isocitrate dehydrogenase; *AUC*, area under the curve; *VFA*, variable flip angle; *Vp*, plasma volume; K^{trans}, volume transfer constant; *Ve*, volume of the extravascular-extracellular space; *IQR*, interquartile range

Parameter	IDH-wt ($n = 12$) vs. IDH-mut ($n = 29$) (AUC)		AUC comparison DeLong's test (p values)	IDH-mut and 1p19q codeleted ($n = 16$) vs. IDH-mut and 1p19q not-codeleted ($n = 13$) (AUC)		AUC comparison DeLong's test (p values)
	Fixed T1	VFA		Fixed T1	VFA	
Vp						
Mean	.575	.566	.9471	.563	.582	.8928
Median	.609	.596	.9130	.500	.548	.7936
IQR	.543	.568	.8385	.563	.611	.7190
5th percentile	.591	.593	.9683	.517	.510	.9731
10th percentile	.603	.606	.9750	.510	.534	.8023
25th percentile	.588	.583	.9686	.500	.548	.8022
75th percentile	.609	.595	.9060	.529	.553	.8655
90th percentile	.543	.566	.8599	.563	.582	.8947
95th percentile	.503	.540	.7799	.558	.577	.8916
K^{trans}						
Mean	.580	.546	.7192	.563	.500	.7369
Median	.592	.569	.8105	.567	.577	.9609
IQR	.569	.572	.9757	.543	.524	.9214
5th percentile	.514	.557	.8282	.625	.591	.8077
10th percentile	.509	.534	.8911	.548	.596	.7242
25th percentile	.534	.546	.9112	.500	.649	.2602
75th percentile	.578	.580	.9759	.543	.548	.9804
90th percentile	.546	.546	1.000	.524	.519	.9800
95th percentile	.546	.540	.9506	.553	.505	.7389
Ve						
Mean	.586	.552	.7454	.529	.587	.7624
Median	.543	.557	.8896	.577	.524	.7874
IQR	.555	.572	.8713	.558	.538	.9243
5th percentile	.625	.506	.0267	.500	.567	.3751
10th percentile	.568	.543	.4740	.587	.567	.8037
25th percentile	.599	.569	.7296	.654	.567	.4121
75th percentile	.563	.576	.9055	.558	.538	.9238
90th percentile	.523	.537	.8924	.538	.606	.7346
95th percentile	.503	.509	.9565	.505	.591	.6607

mut gliomas with and without 1p19q codeletion, the AUC ranged from 0.500 to 0.654 (Table 4) with no statistically significant differences among parameters.

Discussion

In this study, we show that DCE-MRI perfusion parameters obtained with different prebolus T1 measurements are significantly different and that the use of T1 mapping obtained with the VFA method does not improve the diagnostic accuracy of DCE-MRI when compared with the use of a fixed T1 value.

The histogram parameters compared with the Wilcoxon test are significantly different for all the perfusion metrics, except for the 10th and 25th percentiles of Ve in the LGG group, which is not unexpected since these metrics are usually close to zero (or zero) in LGG (Table. 2; Figs. 3, 5, and 6).

Bland-Altman analysis confirmed this finding and shows that perfusion parameters obtained with the fixed T1 method are consistently higher than those obtained with the T1 mapping, as the biases are always positive (Fig. 4 and Electronic

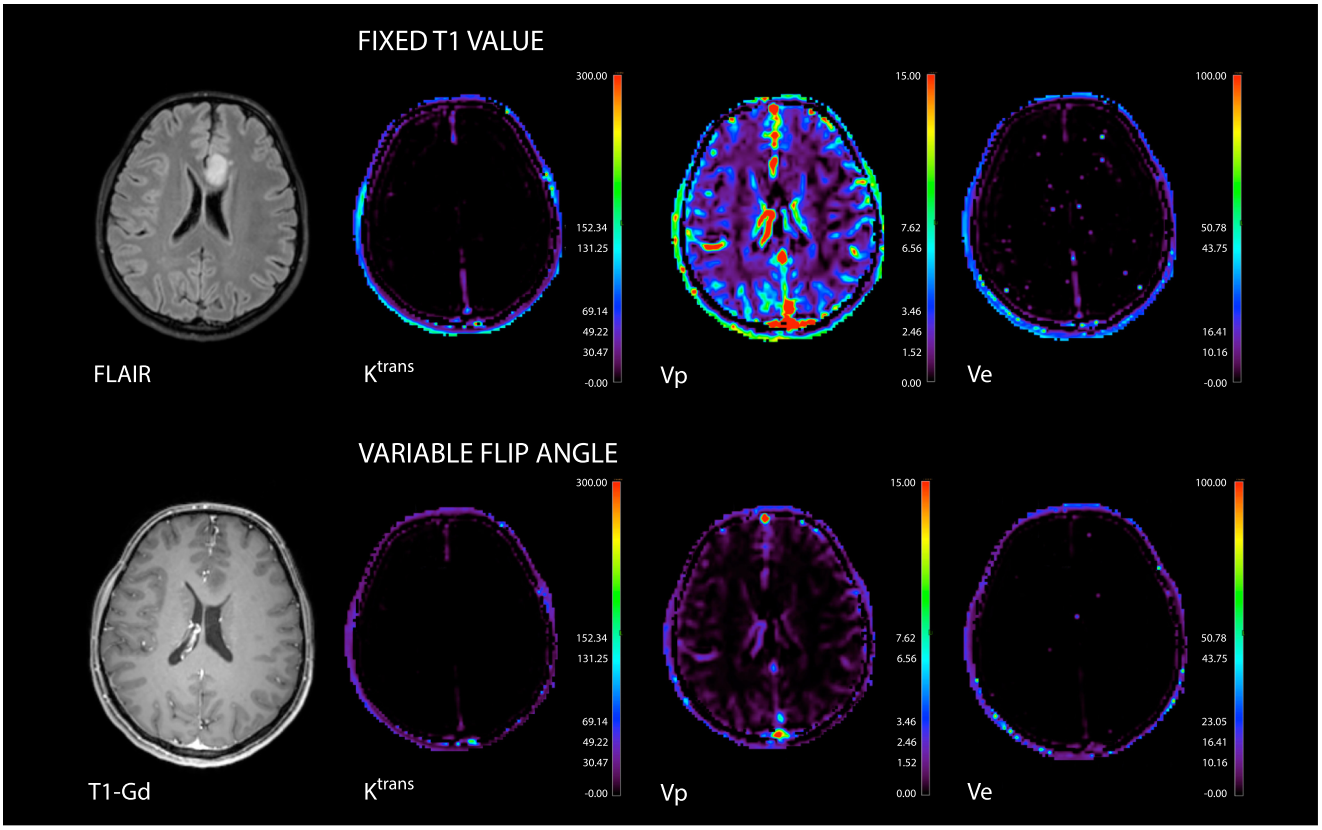

Fig. 5 A case of diffuse astrocytoma (WHO grade II). Perfusion maps of K^{trans}, Vp, and Ve were obtained applying a fixed T1 value and the T1 mapping by variable flip angle. Maps obtained with the fixed T1 value show higher perfusion parameters (perfusion maps are shown to the same scale). Vp, plasma volume; K^{trans}, volume transfer constant; Ve, volume of the extravascular-extracellular space

Supplementary Material 1–6). Moreover, the difference between the two methods seems to increase for increasing values of the perfusion metrics. These findings are consistent in both LGG and HGG groups, except for the 5th and 10th percentiles of Ve in the LGG group, and in line with already published data [8].

These findings have at least two significant consequences on the application of perfusion analysis in clinical practice and research. First, perfusion data obtained from cohorts of patients using a different prebolus T1 measurement should not be considered together. If the T1 mapping method has been selected but is not acquired in a subject, that subject should be excluded from the study since the perfusion data obtained applying a fixed T1 value would be on a different scale compared with the rest of the cohort. Secondly, all published data (i.e. cutoff value used to discriminate between lower- and high-grade gliomas) are specific to the prebolus T1 measurement applied and cannot be extended to a cohort of patients for which a different method has been used.

Concerning the diagnostic accuracy for glioma grading and molecular profiling, we found that the two methods are substantially equivalent since all comparisons show no significant differences in ROC curve values except for few histogram parameters (Tables 3 and 4, Electronic Supplementary Material 7). The observed differences favoured the two prebolus estimation methods equally and without showing a clear trend, suggesting that the observed results may be due to random effects rather than to substantial differences between the two methods.

As regards molecular profiling, 97% of the GBMs in our cohort of patients were IDH-wt. In order to address any confounding factor due to this class imbalance, we performed two separate analyses: one including only grade II and grade III gliomas and one including also GBMs. We believe that the higher accuracy found in the latter analysis reflects the ability of DCE-MRI to discriminate lower-grade gliomas from GBMs rather than IDH-wt from IDH-mut gliomas and may be a consequence of the class imbalance (Table 4 and Electronic Supplementary Material 7). However, the two prebolus estimation methods performed equally in both cases.

Tietze et al [8] demonstrated that the prebolus T1 measurement using VFA is a potential source of errors, also showing that the VFA method is not superior to a fixed prebolus T1 value in glioma grading in a small cohort of patients. It must be emphasised that both those and our

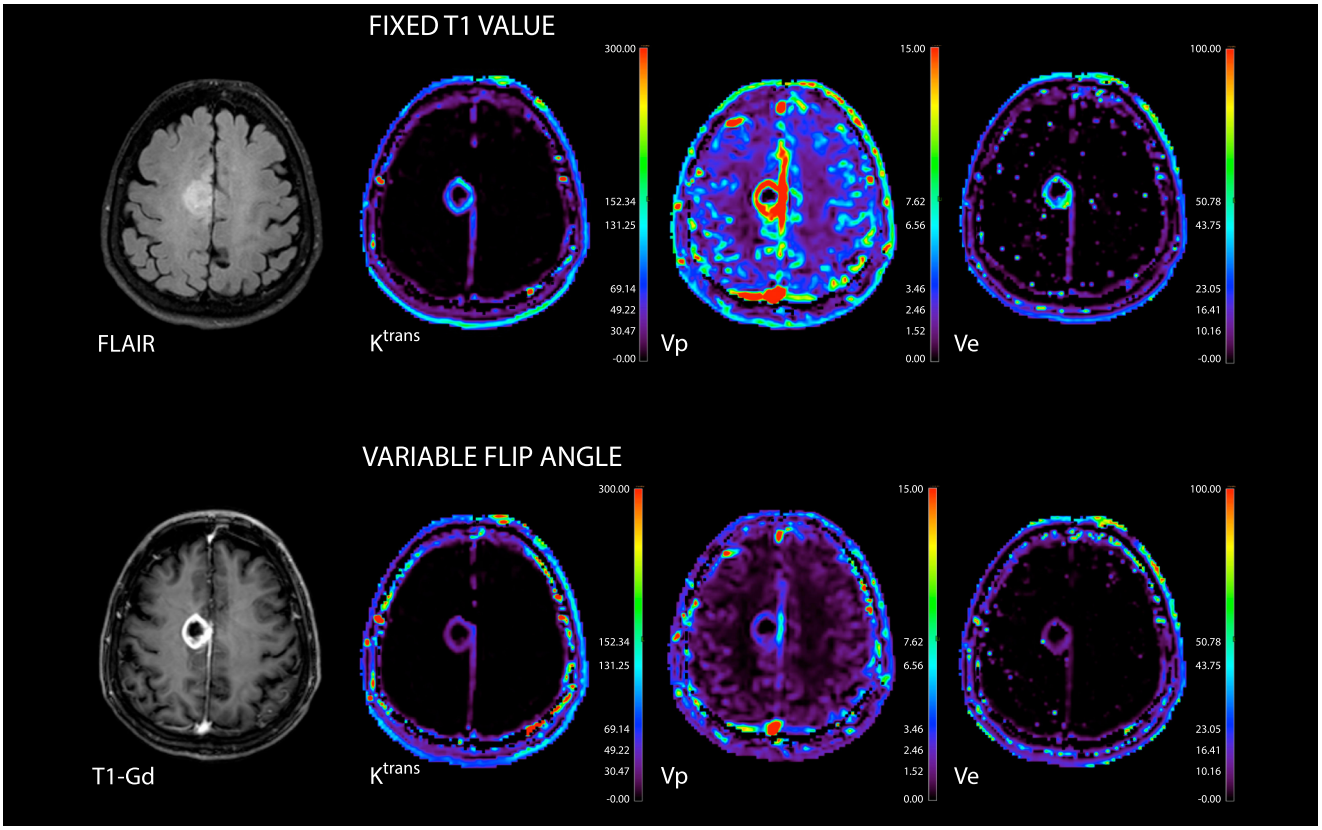

Fig. 6 A case of a glioblastoma (WHO grade IV). Perfusion maps of K^{trans}, Vp, and Ve were obtained applying a fixed T1 value and the T1 mapping by variable flip angle. Maps obtained with the fixed T1 value show higher perfusion parameters (perfusion maps are shown to the same scale). Vp, plasma volume; K^{trans}, volume transfer constant; Ve, volume of the extravascular-extracellular space

results do not prove the fixed T1 method to be superior to the VFA, as shown by the non-significant differences in the AUC of ROC curve analysis for most of the parameters (Tables 3 and 4). However, the VFA method is a potential source of error and it does not add practical advantages when compared with a fixed T1 value. Moreover, the B1 correction may be challenging in routine clinical practice [8]. Our study confirms Tietze's findings and provides more robust results as we performed our analyses on more extensive and comprehensive dataset inclusive of all glioma grades.

Recently, Nam et al [19] compared the use of a fixed T1 value and a measured T1 in the differentiation of true progression versus pseudoprogression in a group of glioblastomas treated with concurrent radiation therapy and temozolomide chemotherapy, concluding that the use of a fixed T1 value is preferable as it reached higher diagnostic accuracy.

Taken all together, our findings and those already published show that T1 mapping may not be necessary for glioma grading, molecular profiling, and follow-up. Nonetheless, further studies are needed to verify if this is generalizable to other clinical applications of DCE-MRI (i.e. differential diagnosis or definition of response to therapies).

The use of T1 mapping, in addition to being a source of error, is also a potential obstacle to the standardisation and broader use of DCE-MRI in clinical practice. The only current indication is to use two to seven different flip angles, as stated in the evidence- and consensus-based standard document published by the QIBA (Quantitative Imaging Biomarkers Alliance) [23].

In general, while the advantages of quantification are clear, it is not clear why an *absolute* quantification should be pursued if it is technically challenging, is less reproducible, and does not add substantial advantages in terms of diagnostic accuracy. In our opinion, future efforts on the standardisation of DCE-MRI protocol should focus on the use of a fixed T1 value as a valid alternative to T1 mapping techniques, ideally in a large multi-centric and multi-purpose study.

This study has some limitations. First, no B1 field heterogeneity correction was applied to the VFA data. We did not include this step in the study design because it is time-consuming and may not achieve a complete correction [8], making it hardly feasible in clinical practice.

It is possible that a higher diagnostic accuracy could have been achieved with the VFA if this correction had been applied. Nevertheless, the only published paper that

compared DCE-MRI accuracy in glioma grading with and without B1 correction did not find any significative difference [24]. So while it is clear that performing B1 correction in simulated data helps to obtain more accurate measurements [8, 24], its usefulness in clinical data is yet to be proven.

Second, despite following the only current indication for DCE-MRI acquisition for TE and TR [23], the relatively low temporal resolution may have affected Vp measurement. As a result of short TR, despite the use of spoiling gradients, we used a relatively small flip angle. This may have led to potential saturation effects [23].

In conclusion, this study shows that DCE-MRI data obtained with different prebolus T1 are not comparable and that the definition of a prebolus T1 by T1 mapping is not mandatory since it does not improve the diagnostic accuracy of DCE-MRI when compared with the use of a fixed T1 value.

Acknowledgements The authors thank Marcello Cadioli and Antonella Iadanza for technical support, and Bradley J. Erickson for reviewing the article.

Funding The authors state that this work has not received any funding.

Compliance with ethical standards

Guarantor The scientific guarantor of this publication is Nicoletta Anzalone.

Conflict of interest The authors of this manuscript declare relationships with the following companies: Nicoletta Anzalone is a member of the advisory board of Bracco; is a consultant for Bayer Healthcare; is on the speakers bureaus of Bayer Healthcare and Guerbet.

Statistics and biometry No complex statistical methods were necessary for this paper.

Informed consent Written informed consent was obtained from all subjects (patients) in this study.

Ethical approval Institutional Review Board approval was obtained.

Study subjects or cohorts overlap All study subjects have been previously reported in: Anzalone N, Castellano A, Cadioli M, Conte GM, et al. Brain Gliomas: Multicenter Standardized Assessment of Dynamic Contrast-enhanced and Dynamic Susceptibility Contrast MR Images. Radiology, 2018.

Methodology
- retrospective
- diagnostic study
- multicentre study

References

1. Anzalone N, Castellano A, Cadioli M et al (2018) Brain gliomas: multicenter standardized assessment of dynamic contrast-enhanced and dynamic susceptibility contrast MR images. Radiology 287(3): 933–943. https://doi.org/10.1148/radiol.2017170362
2. Nguyen TB, Cron GO, Perdrizet K et al (2015) Comparison of the diagnostic accuracy of DSC- and dynamic contrastenhanced MRI in the preoperative grading of astrocytomas. AJNR Am J Neuroradiol 36:2017–2022. https://doi.org/10.3174/ajnr.A4398
3. Taunk NK, Oh JH, Shukla-Dave A et al (2017) Early post-treatment assessment of MRI perfusion biomarkers can predict long-term response of lung cancer brain metastases to stereotactic radiosurgery. Neuro Oncol 20(4):567–575. https://doi.org/10.1093/neuonc/nox159
4. Abe T, Mizobuchi Y, Nakajima K et al (2015) Diagnosis of brain tumors using dynamic contrast-enhanced perfusion imaging with a short acquisition time. Springerplus 4:1–6. https://doi.org/10.1186/s40064-015-0861-6
5. Ulyte A, Katsaros VK, Liouta E et al (2016) Prognostic value of preoperative dynamic contrast-enhanced MRI perfusion parameters for high-grade glioma patients. Neuroradiology 58:1197–1208. https://doi.org/10.1007/s00234-016-1741-7
6. Yoo RE, Choi SH, Kim TM et al (2017) Dynamic contrast-enhanced MR imaging in predicting progression of enhancing lesions persisting after standard treatment in glioblastoma patients: a prospective study. Eur Radiol 27:3156–3166. https://doi.org/10.1007/s00330-016-4692-9
7. O'Connor JP, Tofts PS, Miles KA, Parkes LM, Thompson G, Jackson A (2011) Dynamic contrast-enhanced imaging techniques: CT and MRI. Br J Radiol 84 Spec No 2:S112–20. https://doi.org/10.1259/bjr/55166688
8. Tietze A, Mouridsen K, Mikkelsen IK (2015) The impact of reliable prebolus T 1 measurements or a fixed T 1 value in the assessment of glioma patients with dynamic contrast enhancing MRI. Neuroradiology 57:561–572. https://doi.org/10.1007/s00234-015-1502-z
9. Heye AK, Thrippleton MJ, Armitage PA et al (2016) Tracer kinetic modelling for DCE-MRI quantification of subtle blood–brain barrier permeability. Neuroimage 125:446–455. https://doi.org/10.1016/j.neuroimage.2015.10.018
10. Ellingson BM, Bendszus M, Sorensen AG, Pope WB (2014) Emerging techniques and technologies in brain tumor imaging. Neuro Oncol 16:vii12–vii23. https://doi.org/10.1093/neuonc/nou221
11. Dale BM, Jesberger JA, Lewin JS, Hillenbrand CM, Duerk JL (2003) Determining and optimizing the precision of quantitative measurements of perfusion from dynamic contrast enhanced MRI. J Magn Reson Imaging 18:575–584. https://doi.org/10.1002/jmri.10399
12. Conte GM, Castellano A, Altabella L et al (2017) Reproducibility of dynamic contrast-enhanced MRI and dynamic susceptibility contrast MRI in the study of brain gliomas: a comparison of data obtained using different commercial software. Radiol Med 122:294–302. https://doi.org/10.1007/s11547-016-0720-8
13. Jahng GH, Stables L, Ebel A et al (2005) Sensitive and fast T1 mapping based on two inversion recovery images and a reference image. Med Phys 32:1524–1528. https://doi.org/10.1118/1.1915014
14. Henderson E, McKinnon G, Lee TY, Rutt BK (1999) A fast 3D Look-Locker method for volumetric T1 mapping. Magn Reson Imaging 17:1163–1171. https://doi.org/10.1016/S0730-725X(99)00025-9
15. Fram EK, Herfkens RJ, Johnson GA et al (1987) Rapid calculation of T1 using variable flip angle gradient refocused imaging. Magn Reson Imaging 5:201–208. https://doi.org/10.1016/0730-725X(87)90021-X
16. Chang L, Koay C, Basser PJ, Pierpaoli C (2008) Linear least-squares method for unbiased estimation of T1 from SPGR signals. Magn Reson Med 60:496–501. https://doi.org/10.1002/mrm.21669

17. Stikov N, Boudreau M, Levesque IR, Tardif CL, Barral JK, Pike GB (2015) On the accuracy of T1 mapping: searching for common ground. Magn Reson Med 73:514–522. https://doi.org/10.1002/mrm.25135
18. Larsson C, Kleppestø M, Grothe I, Vardal J, Bjørnerud A (2015) T1 in high-grade glioma and the influence of different measurement strategies on parameter estimations in DCE-MRI. J Magn Reson Imaging 42:97–104. https://doi.org/10.1002/jmri.24772
19. Nam JG, Kang KM, Choi SH et al (2017) Comparison between the prebolus T1 measurement and the fixed T1 value in dynamic contrast-enhanced MR imaging for the differentiation of true progression from pseudoprogression in glioblastoma treated with concurrent radiation therapy and temozolomide chemotherapy. AJNR Am J Neuroradiol 38:2243–2250. https://doi.org/10.3174/ajnr.A5417
20. Louis DN, Perry A, Reifenberger G et al (2016) The 2016 World Health Organization Classification of Tumors of the Central Nervous System: a summary. Acta Neuropathol 131:803–820. https://doi.org/10.1007/s00401-016-1545-1
21. Mouridsen K, Christensen S, Gyldensted L, Ostergaard L (2006) Automatic selection of arterial input function using cluster analysis. Magn Reson Med 55:524–531. https://doi.org/10.1002/mrm.20759
22. Tofts PS, Brix G, Buckley DL et al (1999) Estimating kinetic parameters from dynamic contrast-enhanced T(1)-weighted MRI of a diffusable tracer: standardized quantities and symbols. J Magn Reson Imaging 10:223–232
23. DCE MRI Technical Committee. DCE MRI Quantification Profile, Quantitative Imaging Biomarkers Alliance. Version 1.0. Reviewed Draft. QIBA, July 1, 2012. Available from: http://qibawiki.rsna.org/index.php/Profiles
24. Sengupta A, Gupta R, Singh A (2017) Evaluation of B1 inhomogeneity effect on DCE-MRI data analysis of brain tumor patients at 3T. J Transl Med 15:242. https://doi.org/10.1186/s12967-017-1349-7